3. J. Patarin, J.-L. Paillaud, H. Kessler, in *Handbook of Porous Solids*, F. Schüth, K. S. W. Sing, J. Weitkamp, Eds. (Wiley, Weinheim, Germany, 2002), vol. 2, pp. 815–876.
4. P. Caullet, J.-L. Guth, J. Hazm, J.-M. Lamblin, H. Gies, *Eur. J. Solid State Inorg. Chem.* **28**, 345 (1991).
5. A. Corma, M. Puche, F. Rey, G. Sankar, S. J. Teat, *Angew. Chem. Int. Ed. Engl.* **42**, 1156 (2003).
6. E. Aubert, F. Porcher, M. Souhassou, V. Petrıcek, C. Lecomte, *J. Phys. Chem. B* **106**, 1110 (2002).
7. P. A. Barrett *et al.*, *Chem. Commun.* **2003**, 2114 (2003).
8. A. Corma, M. T. Navarro, F. Rey, J. Rius, S. Valencia, *Angew. Chem. Int. Ed. Engl.* **40**, 2277 (2001).
9. A. Corma, M. J. Diaz-Cabanas, J. Martinez-Triguero, F. Rey, J. Rius, *Nature* **418**, 514 (2002).
10. A. Corma, F. Rey, S. Valencia, J. L. Jorda, J. Rius, *Nature Mater.* **2**, 493 (2003).
11. A. Corma, M. Navarro, F. Rey, S. Valencia, *Chem. Commun.* **2001**, 1486 (2001).
12. A. Corma, M. J. Diaz-Cabanas, F. Rey, *Chem. Commun.* **2003**, 1050 (2003).
13. M. O'Keeffe, O. M. Yaghi, *Chem. Eur. J.* **5**, 2796 (1999).
14. T. Blasco *et al.*, *J. Phys. Chem. B* **106**, 2634 (2002).
15. J. A. Vidal-Moya, T. Blasco, F. Rey, A. Corma, M. Puche, *Chem. Mater.* **15**, 3921 (2003).
16. Y. Wang, J. Song, H. Gies, *Solid State Sci.* **5**, 1421 (2003).
17. Materials and methods are available as supporting material on *Science* Online.
18. All framework type codes are derived from the names of the type materials and consist of three capital Roman letters. For more information, see Ch. Baerlocher, W. M. Meier, D. H. Olson, *Atlas of Zeolite Framework Types* (Elsevier, Amsterdam, ed. 5, 2001); also available at www.iza-structure.org/databases.
19. C. C. Freyhardt, M. Tsapatsis, R. F. Lobo, K. J. Balkus, M. E. Davis, *Nature* **381**, 295 (1996).
20. M. Yoshikawa *et al.*, *J. Phys. Chem. B* **102**, 7139 (1998).
21. A. Burton *et al.*, *Chem. Eur. J.* **9**, 5737 (2003).
22. K. G. Strohmaier, D. E. W. Vaughan, *J. Am. Chem. Soc.* **125**, 16035 (2003).
23. We thank the Institut Français du Pétrole for providing the germanium source. B.H. thanks the Ministère de l'Education Nationale, de la Recherche et de la Technologie for financial support.

Supporting Online Material

www.sciencemag.org/cgi/content/full/304/5673/990/DC1
Materials and Methods
Figs. S1 to S3
Tables S1 and S2
References

23 March 2004; accepted 8 April 2004

Preference for Vibrational over Translational Energy in a Gas-Surface Reaction

R. R. Smith, D. R. Killelea, D. F. DelSesto, A. L. Utz

State-resolved gas-surface reactivity measurements revealed that vibrational excitation of ν_3 (the antisymmetric C-H stretch) activates methane dissociation more efficiently than does translational energy. Methane molecules in the vibrational ground state require 45 kilojoules per mole (kJ/mol) of translational energy to attain the same reactivity enhancement provided by 36 kJ/mol of ν_3 excitation. This result contradicts a key assumption underlying statistical theories of gas-surface reactivity and provides direct experimental evidence of the central role that vibrational energy can play in activating gas-surface reactions.

A molecule's dissociative adsorption onto a solid surface is central to heterogeneous chemical processes ranging from industrial and environmental catalysis to the vapor deposition of materials. Despite the enormous significance of this chemical event, key questions surround some of its most fundamental aspects. We experimentally addressed one of those questions by asking whether energy flows freely between a reagent's translational and vibrational degrees of freedom during reaction. We examined the reactivity of methane (CH_4) incident on a clean nickel surface. This reaction step is rate-limiting in the chief industrial process used for hydrogen production. We compared the efficacy of energy selectively deposited into vibrational motion (the ν_3 antisymmetric C-H stretch) with that deposited into translational motion of the molecule toward the surface. In contrast to prior state-resolved studies of gas-surface reactivity, we found unambiguous evidence that vibrational energy (E_{vib}) is more effective than translational energy (E_{trans}) in promoting reactivity.

Polanyi noted many years ago that dynamical constraints might cause E_{trans} and E_{vib} to differ in their ability to activate a chemical reaction (*1*). On a simple two-dimensional (2D) potential energy surface (PES), when the transition state (TS) lies nearer the entrance channel (the "early barrier"), E_{trans} is most effective in promoting reaction. In contrast, when the TS lies nearer the exit, or product channel (the "late barrier"), E_{vib} is most effective.

When viewed in the context of the Polanyi model, prior beam-surface studies of CH_4 dissociation on Ni(100) and Ni(111) suggested a moderately late barrier, where both E_{trans} and E_{vib} promote reaction (*2*–*5*). Increasing either E_{trans} along the surface normal or the vibrational temperature of the incident CH_4 gas dramatically enhanced reactivity. Collision-induced dissociation studies of CH_4 on Ni(111) further supported the role of vibrational activation in CH_4 dissociation (*6*). These results are also consistent with theoretical predictions of a TS geometry whose elongated C-H bond is bent relative to the C_3 axis of the nonreactive methyl group (*7*).

Many reactions in the gas phase have exhibited a preference for vibrational activation (*8*), but there are no unambiguous experimental examples of this behavior in the field of gas-surface reactivity. Vibrational state–resolved reaction probabilities for H_2 and D_2 on copper found that E_{vib} in H_2 or D_2 was about half as effective as E_{trans} in promoting dissociation (*9*, *10*). Vibrational efficacies greater than 1 have been reported for beam-surface studies of CH_4 dissociation on Ni(111) (*5*), Ni(100) (*3*), and Ru(0001) (*2*), but supporting data are indirect. On Ni(111), experiments that varied the beam source nozzle temperature suggested that E_{vib} was at least as effective as E_{trans} in promoting CH_4 dissociation. Vibrational state averaging in the beam and the difficult nature of the experiments prevented the authors from reaching a more definitive conclusion. On Ni(100) and Ru(0001), the data analysis procedure attributed all vibrational activation to a single diatomic-like C-H oscillator. We find that omitting contributions from the many other vibrational states in CH_4 significantly overestimates the vibrational efficacy of the CH_4 C-H vibration (*11*, *12*).

Vibrational state–resolved measurements of CH_4 dissociation on transition metal surfaces have also not revealed a preference for vibrational activation. Juurlink *et al.* (*12*, *13*) studied the dissociative chemisorption of CH_4 excited to ν_3, $v = 1$, on Ni(100) and found that 36 kJ/mol of E_{vib} was slightly less effective than E_{trans} in promoting reactivity. Schmid *et al.* (*14*) found $2\nu_3$ of CH_4 to be 90% as effective as E_{trans} in promoting reaction on Ni(100), and Higgins *et al.* (*15*) found that $2\nu_3$ excitation in CH_4 was only 40% as effective as E_{trans} in promoting dissociative chemisorption on Pt(111).

State-resolved measurements of N_2 desorption from Ru(0001) used the principle of detailed balance to argue that E_{vib} exceeds E_{trans} in its ability to promote dissociative chemisorption (*16*). Although the authors' model assumes an identical asymptotic (high E_{trans}) reactivity for all N_2 vibrational states, data supporting this assertion are unavailable. Luntz noted that vibrational efficacy correlates to a shift in translational excitation functions along the E_{trans} axis only when the functions have identical shape (slope and as-

Department of Chemistry and W. M. Keck Foundation Laboratory for Materials Chemistry, Tufts University, Medford, MA 02155, USA.

ymptote) (*17*). When the excitation functions differ in shape, they must be more fully characterized to properly assess vibrational efficacy. Additional measurements and analysis by Luntz and co-workers (*18*) suggested that all data for N_2/Ru(0001) were consistent with a vibrational efficacy less than or equal to 1 if asymptotic reactivity increases with vibrational excitation of N_2, as has been reported for H_2/Cu (*9*). Resolution of this controversy awaits state-resolved measurements that reveal the high E_{trans} asymptotic reactivity of N_2 as a function of vibrational state. Our measurements fully characterize the translational excitation functions for CH_4/Ni(111) and overcome this limitation.

Supersonic molecular beams of selectively excited reagent molecules permit a systematic and comparative study of how energy deposited into select energetic degrees of freedom can activate surface chemistry (*12*–*15*, *19*–*23*). We excited CH_4 molecules to $v = 1$, $J = 2$ of ν_3 and quantified the initial reaction probability S_0 on a clean Ni(111) surface as a function of E_{trans} along the surface normal. We then compared the reactivity of CH_4 in its ν_3 and $v = 0$ vibrational states.

We describe key aspects of our experimental approach here and provide additional details in the supporting online material (*24*). Supersonic molecular beams provided CH_4 molecules with a broadly tunable (9.2 to 139 kJ/mol) yet narrow ($\triangle E/E \leq 7\%$) E_{trans} distribution. An infrared (IR) laser selectively excited CH_4 molecules in the beam to a single excited state with a precisely defined E_{vib} and rotational energy. The CH_4 beam impinged on a clean Ni(111) single crystal held at 475 K (*25*). Collision-free conditions in the beam and the long ν_3 IR lifetime ensured that essentially all optically excited molecules reached the surface in their prepared state. The nascent products of CH_4 dissociation on Ni(111) were chemisorbed H and CH_3. At 475 K, adsorbed CH_3 promptly dehydrogenated to C(ad) + 3 H(ad), H(ad) recombinatively desorbed, and chemisorbed C remained to signify a reactive scattering event (*26*). Auger electron spectroscopy quantified the areal density of C resulting from CH_4 dissociation, and a separate measurement quantified the CH_4 flux incident on the surface during the dose. We performed measurements in the limit of low coverage (typically $\theta < 0.08$ monolayer) and computed the ratio of the C atom areal density to the integrated incident flux to obtain S_0.

Our experimental method quantified the average reactivity of all molecules in the molecular beam, including those not excited to ν_3. We have previously shown (*12*) that Eq. 1 relates the ensemble averaged S_0 for molecular beams with ($S_0^{\text{Laser On}}$) and without ($S_0^{\text{Laser Off}}$) laser excitation to the reactivity of the laser excited state $S_0^{\nu_3}$

$$S_0^{\nu_3} = \frac{S_0^{\text{Laser On}} - S_0^{\text{Laser Off}}}{f_{exc}} + S_0^{v=0} \qquad (1)$$

To calculate $S^{0\nu_3}$, we must know the fraction of molecules we excite in the beam (f_{exc}) and the reactivity of the vibrational ground state, $S_0^{v=0}$. Saturation measurements, IR absorption measurements of rotational state populations in the beam, and knowledge of the limiting excitation probability under saturation conditions define f_{exc}, which ranges from 9 to 24% in this work (*21*). Values of S_0 measured in experiments that use low nozzle source temperatures have little contribution from thermally populated vibrationally excited states in the beam and serve as an upper limit on $S_0^{v=0}$. We are currently performing a detailed analysis of the nozzle temperature dependence of S_0 over a broad range of E_{trans} and nozzle source conditions to obtain a direct estimate of $S_0^{v=0}$ versus E_{trans} (*11*). This analysis will provide values of $S_0^{v=0}$ at higher E_{trans}.

We plot $S_0^{\nu_3}$ and $S_0^{\text{Laser Off}}$ as a function of E_{trans} in Fig. 1. Error bars are 95% confidence limits and include standard deviations observed in replicate measurements as well as our estimates of uncertainty in f_{exc}. The data show that a single vibrational quantum in ν_3 increases S_0 significantly at all E_{trans} studied. The enhancement is largest at low E_{trans}, where the system is most "starved" for the energy that vibrational excitation provides. At E_{trans} = 140 kJ/mol, molecules in the ν_3 state are about 10 times more reactive than are molecules in $v = 0$, but at E_{trans} = 42 kJ/mol, the measured enhancement increases to a factor of 750. Our $S_0^{v=0}$ estimate (*11*) suggests that ν_3 excitation may yield as much as a 7000-fold reactivity enhancement at E_{trans} = 9 kJ/mol.

Curves drawn through each data set in Fig. 1 follow the ansatz of Michelsen *et al.* and permit a comparison of how E_{vib} and E_{trans} compare in their ability to promote reaction (*9*, *17*). The $S_0^{\nu_3}$ curve is the best-fit error function whose asymptote is constrained to unit reactivity at infinitely high E_{trans}. A second error function with the same shape and asymptote as the ν_3 curve is shifted horizontally along the E_{trans} axis by 45 kJ/mol to pass through $S_0^{\text{Laser Off}}$. The arrows in Fig. 1 show that the energy shift between the two curves is constant at several values of S_0, which validates our use of this E_{trans} shift as a measure of vibrational efficacy (*17*). Because $S_0^{\text{Laser Off}}$ is an upper limit on $S_0^{v=0}$, the E_{trans} shift between $S_0^{\nu_3}$ and $S_0^{v=0}$ is slightly larger than that shown. Preliminary results from our detailed analysis of $S_0^{v=0}$ point to an energy shift between $S_0^{\nu_3}$ and $S_0^{v=0}$ that is 1 to 2 kJ/mol greater than the 45 kJ/mol shown in Fig. 1 (*11*). A comparison of the experimentally measured E_{trans} shift and the 36 kJ/mol vibrational quantum we excited reveals that ν_3 excitation is 25% more effective at promoting the dissociative chemisorption of CH_4 on Ni(111) than is E_{trans} directed along the surface normal. This result has important implications for the microscopic details of gas-surface reactions.

It is significant that a single quantum of ν_3 C-H stretch in CH_4 so effectively promotes reactivity on a metal surface. Vibrational relaxation on metal surfaces can be highly efficient, and quenching competes with the activation of dissociative chemisorption (*27*). Theoretical studies suggest that ν_3 may not even be the most reactive of methane's vibrationally excited states. Milot and Jansen's wavepacket calculations predict the ν_1 symmetric C-H stretch state to be more reactive than ν_3 (*28*). More recently, Halonen *et al.* (*29*) performed a normal-modes analysis of the incident molecule as a function of distance above the surface. If dissociation is vibrationally adiabatic, then they too predict that ν_1 is more reactive than ν_3.

Statistical theories of gas-surface reactivity using microcanonical unimolecular rate theory (MURT) predict that reactive complexes containing identical quantities of energy react with equal probability (*30*). This prediction follows directly from the assumption that energy redistribution among participating degrees of freedom is rapid relative to the time of reaction. However, recent studies of CH_2D_2 dissociation on a metal surface (*31*, *32*) have shown that S_0 differs significantly for two combination vibrations containing nearly identical E_{vib}. The vibrational mode specificity exhibited in that work reveals that energy flow among the vibrational degrees of

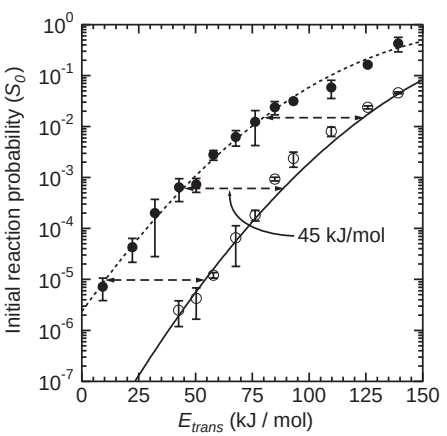

Fig. 1. Reaction probabilities for ν_3, $v = 1$, $J = 2$ ($S_0^{\nu_3}$, solid circles and dashed curve), $S_0^{\text{Laser Off}}$ (open symbols), and an estimate of $S_0^{v=0}$ (solid curve). $S_0^{\text{Laser Off}}$ includes contributions from excited vibrational states thermally populated in the beam and lies above $S_0^{v=0}$, particularly at $E_{trans} > 75$ kJ/mol. The E_{trans} shift between the two reaction probability curves is indicated by the horizontal dashed lines and is equal to 45 kJ/mol at all reaction probabilities.

freedom studied is not sufficiently fast to fulfill the energy redistribution requirements of a statistical model.

The data presented here are also not consistent with predictions from the MURT model, because they show that energy flow between vibrational and translational degrees of freedom is not statistical on the time scale of dissociative chemisorption. Both $v = 0$ and ν_3 data sets were obtained at a surface temperature of 475 K, where surface phonon contributions are identical and relatively small. Extensive rotational cooling in the $v = 0$ beam and state selection ($J = 2$) in the ν_3 beam result in nearly identical and extremely small energetic contributions from CH_4 rotational degrees of freedom. State selection defines E_{vib} with high precision, and we measure the E_{trans} distribution in our beams to be less than 7% (full width at half maximum). In comparing the reactivity of ν_3 and $v = 0$, we find that two ensembles of molecules containing the same total energy do not share the same reaction probability. Removing 36 kJ/mol of energy in the ν_3 coordinate requires the addition of 45 kJ/mol of E_{trans} directed along the surface normal in order to maintain a constant degree of reactivity. In contrast, the application of MURT predicts equal efficacy for these two energetic coordinates (*30*).

We can begin to understand how dynamical constraints lead to nonstatistical behavior by considering how E_{vib} can exceed E_{trans} in its ability to promote dissociative chemisorption (*33*). If dissociation is vibrationally adiabatic, trajectories starting in $v = 0$ must follow the minimum energy pathway through the multidimensional PES, as shown in Fig. 2A. Molecules following this path require a minimum energy of $E_a^{v=0}$ to react, which can come from reagent translation or the thermal bath of the surface. A vibrationally adiabatic trajectory originating in $v = 1$ cannot access a TS energy less than that of the $v = 0$ trajectory. In the limiting case where vibrational excitation projects completely onto the reaction coordinate, the minimum energy for reaction decreases by E_{vib}. Reagent translation and the surface need only provide $E_a^{v=0} - E_{vib}$ of energy, which reduces the E_{trans} requirement by E_{vib}. The vibrational coordinate does not generally map directly onto the reaction coordinate, so less than the full E_{vib} is available for promoting reaction. In no case can vibrational excitation reduce the E_{trans} requirement by more than E_{vib}.

Two explanations involving nickel lattice motion can yield vibrational efficacies greater than 1 within a vibrationally adiabatic picture. We measure vibrational efficacy by quantifying the shift along the E_{trans} axis of the state-resolved reactivity curves for $v = 0$ and ν_3. Because the $v = 0$ curve appears at higher E_{trans}, energy quenching due to lattice recoil may be more significant for $v = 0$ molecules than for ν_3 molecules (*17*). This effect leads to a higher E_{trans} requirement for the $v = 0$ molecules. It is also possible that each CH_4 vibration differs in its coupling with lattice motion. Such an effect could translate into differing abilities to transfer energy into or access energy stored in the nickel lattice (*28*).

Our data are also consistent with a vibrationally nonadiabatic picture where trajectories starting in $v = 0$ do not access the minimum TS energy. Figure 2B follows Polanyi's analysis and shows that trajectories starting in $v = 1$ and surmounting a "late" barrier may access phase space regions where the minimum TS energies are ΔE^* lower than those accessed by trajectories originating in $v = 0$. Effective barrier heights for $v = 0$ and $v = 1$ molecules now differ in two ways. Molecules in $v = 1$ start with more internal energy and access TS configurations whose energy is ΔE^* less than those accessed by $v = 0$ trajectories. These two factors combine and reduce the E_{trans} requirement for $v = 1$ reactivity by ($E_{vib} + \Delta E^*$), which can exceed E_{vib}. Figure 3 shows schematically how the trajectories in Fig. 2B differ in their path along the z and reactive C-H stretch coordinate. Our data point to a PES topology in which ν_3 ($v = 1$) molecules access TS regions whose energy is lower than those accessible by $v = 0$ molecules. Alternatively stated, $v = 0$ molecules cannot access the portion of phase space containing the minimum TS energy.

Our results and those of Beck *et al.* (*31*) illustrate the importance and complexity of excited-state vibrational dynamics in dissociative chemisorption on metals, a situation that presents both challenges and rewards. On one hand, the need to treat reaction dynamics including many degrees of freedom significantly complicates computational and experimental studies. On the other hand, this same complexity offers new opportunities for controlling the outcome of technologically important gas-surface reactions.

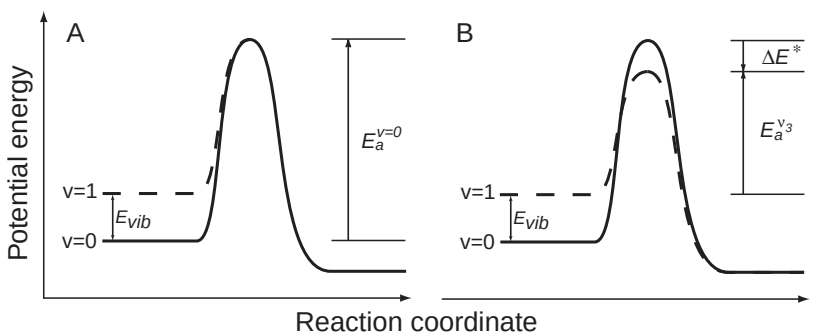

Fig. 2. Reaction path energetics for molecules initially in the $v = 0$ and $v = 1$ vibrational states. The curves represent cuts through the multidimensional PES governing reactivity. (**A**) Limiting adiabatic case: Both reagents access a TS with the same energy. (**B**) Vibrationally nonadiabatic case: $v = 1$ molecules access a lower-energy TS than do those originating in $v = 0$.

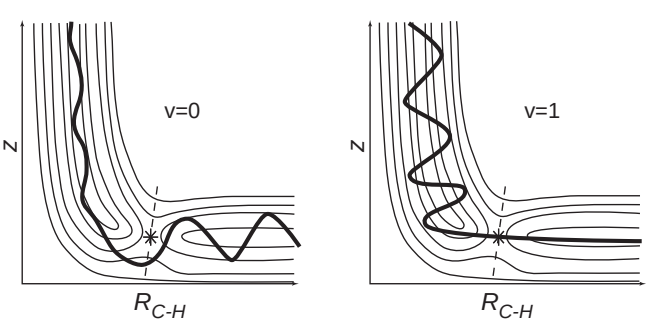

Fig. 3. Schematic 2D PES showing reactive trajectories for $v = 0$ and $v = 1$ molecules as illustrated in Fig. 2B. CH_4 molecules approach the surface along the z coordinate, traverse the TS (dashed line), and proceed on to products (extended C-H distance, R_{C-H}). The TS is a saddle point in the PES, and the minimum TS energy is denoted by an asterisk.

References and Notes

1. J. C. Polanyi, *Acct. Chem. Res.* **5**, 161 (1972).
2. J. H. Larsen, I. Chorkendorff, *Surf. Sci. Rep.* **35**, 165 (1999).
3. P. M. Holmblad, J. Wambach, I. Chorkendorff, *J. Chem. Phys.* **102**, 8255 (1995).
4. A. C. Luntz, *J. Chem. Phys.* **102**, 8264 (1995).
5. M. B. Lee, Q. Y. Yang, S. T. Ceyer, *J. Chem. Phys.* **87**, 2724 (1987).
6. J. D. Beckerle, A. D. Johnson, Q. Y. Yang, S. T. Ceyer, *J. Chem. Phys.* **91**, 5756 (1989).
7. P. Kratzer, B. Hammer, J. K. Nørskov, *J. Chem. Phys.* **105**, 5595 (1996).
8. R. D. Levine, R. B. Bernstein, *Molecular Reaction Dynamics and Chemical Reactivity* (Oxford Univ. Press, New York, 1987).
9. H. A. Michelsen, C. T. Rettner, D. J. Auerbach, R. N. Zare, *J. Chem. Phys.* **98**, 8294 (1993).
10. C. T. Rettner, H. A. Michelsen, D. J. Auerbach, *J. Chem. Phys.* **102**, 4625 (1995).
11. D. F. DelSesto, R. R. Smith, L. B. F. Juurlink, D. R. Killelea, A. L. Utz, in preparation.
12. L. B. F. Juurlink, P. R. McCabe, R. R. Smith, C. L. DiCologero, A. L. Utz, *Phys. Rev. Lett.* **83**, 868 (1999).
13. L. B. F. Juurlink, R. R. Smith, A. L. Utz, *Trans. Faraday Soc.* **117**, 147 (2000).
14. M. P. Schmid, P. Maroni, R. D. Beck, T. R. Rizzo, *J. Chem. Phys.* **117**, 8603 (2002).

15. J. Higgins, A. Conjusteau, G. Scoles, S. L. Bernasek, *J. Chem. Phys.* **114**, 5277 (2001).
16. M. J. Murphy, J. F. Skelly, A. Hodgson, B. Hammer, *J. Chem. Phys.* **110**, 6954 (1999).
17. A. C. Luntz, *J. Chem. Phys.* **113**, 6901 (2000).
18. L. Diekhoner *et al.*, *J. Chem. Phys.* **115**, 9028 (2001).
19. D. C. Jacobs, *J. Phys. Condens. Matter* **7**, 1023 (1995).
20. G. O. Sitz, *Rep. Progr. Phys.* **65**, 1165 (2002).
21. P. R. McCabe, L. B. F. Juurlink, A. L. Utz, *Rev. Sci. Instrum.* **71**, 42 (2000).
22. H. Hou *et al.*, *Science* **284**, 1647 (1999).
23. M. Gostein, G. O. Sitz, *J. Chem. Phys.* **106**, 7378 (1997).
24. Details are available on *Science* Online.
25. K. Christmann, O. Schober, G. Ertl, M. Neumann, *J. Chem. Phys.* **60**, 4528 (1974).
26. Q. Y. Yang, K. J. Maynard, A. D. Johnson, S. T. Ceyer, *J. Chem. Phys.* **102**, 7734 (1995).
27. J. D. Beckerle, M. P. Casassa, R. R. Cavanagh, E. J. Heilweil, J. C. Stephenson, *Phys. Rev. Lett.* **64**, 2090 (1990).
28. R. Milot, A. P. J. Jansen, *Phys. Rev. B* **61**, 15657 (2000).
29. L. Halonen, S. L. Bernasek, D. J. Nesbitt, *J. Chem. Phys.* **115**, 5611 (2001).
30. A. Bukoski, I. Harrison, *J. Chem. Phys.* **118**, 9762 (2003).
31. R. D. Beck *et al.*, *Science* **302**, 98 (2003).
32. A. C. Luntz, *Science* **302**, 70 (2003).
33. H. Mortensen, L. Diekhoner, A. Baurichter, A. C. Luntz, *J. Chem. Phys.* **116**, 5781 (2002).
34. Supported by NSF (grant CHE-0111446) and Tufts University.

Supporting Online Material
www.sciencemag.org/cgi/content/full/304/5673/992/DC1
Materials and Methods

2 February 2004; accepted 5 April 2004

The Structure of the First Coordination Shell in Liquid Water

Ph. Wernet,[1,2] D. Nordlund,[3] U. Bergmann,[1] M. Cavalleri,[3] M. Odelius,[3] H. Ogasawara,[1,3] L. Å. Näslund,[1,3] T. K. Hirsch,[4] L. Ojamäe,[5] P. Glatzel,[6] L. G. M. Pettersson,[3] A. Nilsson[1,3]*

X-ray absorption spectroscopy and x-ray Raman scattering were used to probe the molecular arrangement in the first coordination shell of liquid water. The local structure is characterized by comparison with bulk and surface of ordinary hexagonal ice Ih and with calculated spectra. Most molecules in liquid water are in two hydrogen–bonded configurations with one strong donor and one strong acceptor hydrogen bond in contrast to the four hydrogen–bonded tetrahedral structure in ice. Upon heating from 25°C to 90°C, 5 to 10% of the molecules change from tetrahedral environments to two hydrogen–bonded configurations. Our findings are consistent with neutron and x-ray diffraction data, and combining the results sets a strong limit for possible local structure distributions in liquid water. Serious discrepancies with structures based on current molecular dynamics simulations are observed.

Experimental studies of the hydrogen-bonded network structure in water have mainly relied on neutron and x-ray diffraction and infrared (IR) spectroscopies (*1*). Diffraction data from noncrystalline materials provide radial distribution functions (RDFs) (*2*–*4*) that do not provide angular correlations needed to uniquely assign local geometries in water (*5*–*7*). A more detailed atomistic picture has been derived theoretically by molecular dynamics (MD) simulations (*4*, *8*) that are consistent with diffraction data. Structural information from IR spectroscopies generally relies on the correlation between the O-H stretching frequency and hydrogen-bond (H-bond) length, which has been shown to be ambiguous for liquid water (*9*).

Here, we report an independent experimental investigation of local bonding configurations in the first coordination shell of liquid water by using the near-edge fine structure in x-ray absorption spectroscopy (XAS), also denoted XANES and NEXAFS, where a core electron is excited into empty electronic states. The character of these states and, hence, the near-edge fine structure in XAS depends on the chemical environment, bond lengths, and bond angles (*10*). We also obtained the same spectral information by using nonresonant x-ray Raman scattering (XRS) involving core excitations (*11*).

XAS and XRS at the oxygen K-edge (*12*) are sensitive to distortions of H-bonds on the H-sides (donor H-bonds) of the molecules in the condensed phases of water (*11*, *13*, *14*). Because the time scale for excitation is much faster than the molecular (vibrational) motions in the liquid, these spectroscopies probe the electronic structure of a distribution of instantaneous configurations and thus allow decomposition in terms of specific H-bond situations (*12*). We analyzed the near-edge structures in the liquid water XA spectrum (the terminology "XA spectrum" is used for both XAS and XRS) with the aid of experimental model systems and calculated spectra. The XA spectra for water molecules in different H-bonding configurations are depicted in Fig. 1, where ice Ih bulk and surface spectra are compared with spectra of bulk liquid water at two temperatures. Bulk ice Ih is tetrahedrally coordinated, but the exact H-bonding environment at the ice Ih surface still raises questions (*15*, *16*). However, there is consensus that a large fraction (50% or more) of the molecules in the first half bilayer of the ice Ih surface has one free O-H group, whereas the other is H-bonded to the second half bilayer. The liquid water XA spectrum closely resembles that for the ice surface, but it is very different from that of bulk ice. We interpret this finding, and our analysis demonstrates that the molecules in the liquid are not predominantly four-coordinated.

The spectra in Fig. 1 can be divided into three main regions: the pre-edge (around 535 eV), the main edge (537 to 538 eV), and the post-edge (540 to 541 eV). The bulk ice spectrum (Fig. 1, curve a) is dominated by intensity in the post-edge region and shows a weak main-edge structure. Both the surface ice (Fig. 1, curve b) and liquid water (Fig. 1, curve d) spectra have a peak in the pre-edge region, a dominant main edge, and less intensity compared with bulk ice in the post-edge region. Termination of the ice surface with NH_3 (Fig. 1, curve c) entails a coordination of the free O-H groups and causes the pre-edge peak to vanish and the intensity to shift to the post-edge region. We assign intensities in the pre- and main-edge regions to water molecules with one uncoordinated O-H group, whereas the intensity in the post-edge region is related to fully coordinated molecules. Remarkably, most molecules in bulk liquid water at room temperature exhibit a local coordination comparable to that at the ice surface, with one strong and one non-, or only weakly, H-bonded O-H group. The contribution to the spectrum from molecules with four-fold coordination similar to bulk ice is very small. Performing the measurements with D_2O or H_2O led to identical spectra within the experimental resolution, and thus tunneling contributions are not decisive.

Comparison of the XRS spectra of room-temperature (25°C) and hot water (90°C) (Fig. 1, curve e) shows that heating increases intensities in the pre- and main-edge regions while decreasing that in the post-edge, but the changes are small compared with the changes observed between ice and the liquid. Figure 1, curve f, shows the difference spectra of 25°C water minus ice (*17*) (solid curve) and 90°C minus 25°C water (circles with error bars). The latter has been multiplied by a factor of 10 to

[1]Stanford Synchrotron Radiation Laboratory, Post Office Box 20450, Stanford, CA 94309, USA. [2]BESSY, Albert-Einstein-Strasse 15, D-12489 Berlin, Germany. [3]FYSIKUM, Stockholm University, AlbaNova, S-10691 Stockholm, Sweden. [4]Department of Physical Chemistry, Stockholm University, S-10691 Stockholm, Sweden. [5]Department of Chemistry, Linköping University, S-58183 Linköping, Sweden. [6]Department of Inorganic Chemistry and Catalysis, Debye Institute, Utrecht University, Sorbonnelaan 16, 3584 CA Utrecht, Netherlands.

*To whom correspondence should be addressed. E-mail: nilsson@slac.stanford.edu